

**G. Hasanova** 

Baku State University, Baku, Azerbaijan

e-mail: gunaiita@gmail.com

## STRUCTURAL AND THERMAL STABILITY OF AG NANOPARTICLES SYNTHESIZED FROM ARTEMISIA LERCHIANA: SEM, EDX, XRD AND TG-DTA ANALYSES

### Abstract

The development of biologically mediated green synthesis of silver nanoparticles (AgNPs) has gained significant global attention due to its promising applications in medical science and disease treatment. Unlike conventional chemical and physical methods, green synthesis employs eco-friendly, non-toxic, and cost-effective approaches, utilizing biological resources such as plants, microorganisms, and natural extracts as reducing and stabilizing agents. In this context, the present study highlights the synthesis of silver nanomaterials using *Artemisia lerchiana* Web. extract as a novel and sustainable source. Compared to conventional antibiotics and chemically synthesized drugs, AgNPs obtained from green routes exhibit remarkable antibacterial, anticancer, antifungal, and anti-inflammatory activities, thereby offering potential solutions to pressing medical challenges such as antibiotic resistance, chronic infections, and tumor progression. The structural and morphological properties of the synthesized nanoparticles were systematically characterized using scanning and transmission electron microscopy (SEM and TEM), energy-dispersive X-ray analysis (EDX), X-ray diffraction (XRD), thermogravimetric-differential thermal analysis (TG-DTA), and zeta potential measurements. These results revealed that the biosynthesized AgNPs possess well-defined size, shape, crystallinity, and homogeneous distribution, which are strongly influenced by the phytochemical composition of the plant extract. Furthermore, this review provides an overview of recent advances in green synthesis strategies, emphasizing the role of biocompatibility in reducing nanoparticle toxicity, minimizing environmental risks, and lowering production costs. The findings confirm that biologically synthesized silver nanoparticles represent a promising alternative to conventional nanomaterials for biomedical and pharmaceutical applications, with enhanced safety profiles, stability, and therapeutic efficiency. This work contributes to the growing body of research focused on eco-friendly nanotechnology for sustainable and advanced healthcare solutions.

**Keywords:** AgNP, green synthesis, SEM-TEM, EDX, XRD, TG-DTA, Zeta potential.

### Introduction

Nanobiotechnology is a promising field that studies the structure and practice of nanoparticles (NPs) in many fields (Sunderam et., 2019). The unique properties of nanoparticles are based on their monodisperse size and surface morphology; different shapes and sizes can be obtained by changing the synthesis stage of nanomaterials (Clarance, 2020; Hosny, 2021). Nanoparticles are widely produced in industry by physical and chemical methods (Bandeira et., 2020). Nowadays, instead of traditional methods, it is more preferred to produce nanoparticles by fast and cheap green synthesis procedures that do not pollute the environment and do not use toxic solvents (Badeggi et., 2020). In this context, scientific research has focused on synthesizing these nanomaterials from biological sources such as plants, algae,

seaweed, viruses, bacteria, and fungi (Chellamuthu, 2019; Aktepe, 2021).

In nanoparticle research, zinc (Thema et., 2015) gold (Soliman et., 2020), silver (Salem et., 2020), nickel (Pandian et., 2015), iron (Devatha et., 2016), platinum (Thirumurugan et., 2016), and selenium (Cittrarasu et., 2021) salts have been extensively investigated in nanoparticle synthesis.

Due to their unique physical and chemical properties, silver nanoparticles (AgNPs) are increasingly used in various fields, including medicine, food, healthcare, consumer, and industrial applications. These include optical, electrical and thermal, high electrical conductivity and biological properties (Gurunathan, 2015; Li, 2010; Mukherjee, 2001). Due to their unique properties, they are suitable for several applications, including as antibacterial agents in industrial, household and health-related fields, con-

sumer products, medical device coatings, optical sensors and cosmetics, pharmaceutical industry, food industry, diagnostics, orthopedics, drug delivery, anticancer are used as agents (Chernousova&Epple, 2013). Nanoscale metal particles are unique and can significantly change their physical, chemical, and biological properties due to their surface-to-volume ratio; therefore, these nanoparticles have been used for various purposes (Li, 2001; Sharma, 2008). Various methods have been adopted for the synthesis of AgNPs. In general, traditional physical and chemical methods seem to be very expensive and dangerous (Gurunathan, 2015; Kalishwaralal, 2015). Interestingly, biologically prepared AgNPs exhibit high yield, solubility, and high stability (Gurunathan et., 2015). Among several synthetic methods for AgNPs, biological methods are more widely used as simple, rapid, non-toxic, reliable and green approaches.

As an alternative for sustainable development in green nanobiotechnology, environmentally friendly and economically efficient technology is used to reduce toxic waste generated by industrial and chemical processes (Rai, 2013). Nanoparticles (NPs) can be synthesized by physical, chemical and biological methods (Reverberi et., 2019). Physical and chemical synthesis is energy-intensive and in many cases involves toxic substances, while biological methods are more cost-effective, clean, non-toxic and environmentally friendly. Biological synthesis using plant extracts has been proposed as an environmentally friendly alternative compared to other methods (Saravanakumar et., 2017). Plants are widespread, readily available, safe to handle, low production cost, and a source of various metabolites (bioactive phytochemical elements) (Elumalai et., 2010)

Therefore the aim of our study was to investigate the characteristics of silver nanoparticles obtained using the extract of Artemisia lerchiana Web, since the search for the most effective and environmentally safe ways of obtaining NPs still remains a pressing issue.

## Materials and methods

### *Preparation of wormwood extract and silver nitrate (AgNO<sub>3</sub>) solution*

In order to get the plant extract have been used the vegetative organs of Artemisia lerchiana Web. plant samples were collected from Lokbatan settlement of Absheron region of Azerbaijan in the summer season. The samples were washed several times first with tap water and then with distilled water. The leaves of plant samples were dried in room conditions

for 48 hours. 50 g of dried plant leaves were placed in a 500 ml beaker, then 250 ml of distilled water was added, and the mixture was boiled. The mixture is boiled for 5 minutes to get the desired result. Then the extract was cooled to room temperature. Filtering of the plant extract was done with No. 1 Whatman filter paper. The obtained extract was stored at +4 °C until experiments. In order to obtain silver NPs, a solution of silver nitrate was prepared in the following proportion: 25 grams of salt were dissolved in 300 ml of distilled water.

### *Biosynthesis*

50 ml extract of wormwood leaves and 250 ml AgNO<sub>3</sub> solution were placed in a 1000 ml flask and reacted at 45 °C after just shaking by hand. The reaction mixture was found to change color with time. The extract obtained as a result of the reaction was centrifuged at 6000 rpm for 15 minutes with an OHAUS FC 5706 device. After several washings, the precipitated solid was dried in an oven at 75°C for 24 h. The obtained particles were then prepared for characterization. Phytochemicals in plant extracts reduced Ag<sup>+1</sup> to Ag<sup>0</sup>, thus forming AgNPs (Mani et., 2021).

### *Scanning Electron Microscopy (SEM)*

The surface morphology of the synthesized Ag nanoparticles was examined using a Field Emission Scanning Electron Microscope (FESEM, EVO 40 LEQ). Dried nanoparticle powder was mounted on conductive carbon tape and analyzed under high vacuum. Images were collected at 5–15 kV accelerating voltage, depending on resolution requirements. The SEM micrographs were used to assess particle shape, agglomeration behavior, and qualitative size distribution.

### *Transmission Electron Microscopy (TEM)*

Nanoscale morphology and internal structural features were investigated using Transmission Electron Microscopy (TEM, JEOL JEM-1010) operating at 200 kV. A dilute suspension of Ag nanoparticles in ethanol was prepared and ultrasonicated for 10 min to minimize agglomeration. High-resolution TEM (HRTEM) imaging was performed to determine lattice fringes and interplanar spacings. Particle size analysis was conducted using ImageJ software based on measurements of >100 particles.

### *Energy-Dispersive X-ray Spectroscopy (EDX)*

Energy Dispersive X-ray Analysis (EDX) reveals the presence of silver and oxygen elements

in the nanoparticles, which indicates the purity and complete chemical composition of the AgNPs. EDX analysis shows the relative composition of elements such as Oxygen (O), Aluminum (Al), Carbon (C) and Silver (Ag). Other elements are organic substances bound to the surface of the silver nanoparticles (Dada et al., 2017). The percentage of Ag metal found is significant compared to other chemical elements. Red, green and blue spots indicate the presence of silver, oxygen and carbon elements, respectively, in the green synthesized silver nanoparticles. The elemental composition was confirmed using EDX spectroscopy integrated with a FESEM system (Rad B-DMAX II, Japan). The spectra were obtained under high vacuum under optimized beam conditions. The characteristic emission lines of silver ( $\text{Ag } L\alpha \approx 3.0 \text{ keV}$ ) were used to verify the identity of the elements and assess the purity.

#### *X-ray Diffraction (XRD)*

XRD is a technique used to determine both qualitative and quantitative analyzes of nanoparticles. This analyzes are used to confirm the formation of nanoparticles and determine their crystal structure. In addition, this technique was used to calculate the crystalline nanoparticle size and measure the degree of crystallinity. Crystalline structure and phase purity of the Ag nanoparticles were analyzed using X-ray diffraction ((Rad B-DMAX II, Japan) equipped with  $\text{Cu } K\alpha$  radiation ( $\lambda = 1.5406 \text{ \AA}$ ) operating at 40 kV and 15 mA. Diffraction patterns were collected in the  $2\theta$  range of  $20^\circ$ – $80^\circ$  with a scan rate of  $0.02^\circ/\text{s}$ . Average crystallite size was calculated using the Debye–Scherrer equation, based on the FWHM of the and reflections.

#### *Thermogravimetric–Differential Thermal Analysis (TG–DTA)*

Thermal stability was examined using TG–DTA analysis (Shimadzu, Japan). Approximately 8–10 mg of dried nanoparticles was placed in an alumina crucible and heated from  $25^\circ\text{C}$  to  $800^\circ\text{C}$  at a constant rate of  $10^\circ\text{C}/\text{min}$  under a nitrogen atmosphere (flow rate:  $50 \text{ mL}/\text{min}$ ). The TG curve provided information on mass-loss events, while the DTA signal was used to identify associated endothermic and exothermic transitions.

#### *Zeta Potential Analysis*

Colloidal stability and surface charge of the nanoparticle suspension were evaluated using a Zetasizer Nano ZS (Malvern Panalytical, UK) based on electrophoretic light scattering. Nanoparticles were dispersed in deionized water and sonicated for 5 min

prior to analysis. Measurements were performed at  $25^\circ\text{C}$ , and the reported zeta potential represents the mean of three replicate readings. The magnitude of zeta potential was interpreted as an indicator of colloidal stability.

## **Results and discussion**

### *Scanning Electron Microscope (SEM)*

Due to aberration and the limitation of the wavelength of light, it is not possible to achieve additional magnification with optical microscopes. This creates a highly magnified image of the surface or sample.

Silver nanoparticles are very good electrical conductors, making them easy to scan using SEM. Although SEM cannot observe the internal structure of samples, it can provide useful information on particle purity and aggregation (Lavoie, 1995). AgNPs are usually spherical, cubic, triangular, oval, round in shape and appear as single or aggregated particles (Abdellatif et al., 2022). Changes in shape can be caused by changes in synthesis parameters such as pH, temperature and plant concentration.

FE-SEM methods were used to evaluate the size and shape of the silver nanoparticles obtained from the *Artemisia lerchiana* Web. plant extract. As a result of the conducted studies, it was determined that the sizes of AgNPs ranged from 25 to 50 nm and were generally spherical (Fig 1).

In most cases, the obtained particle sizes range from 20 to 30 nm. Thus, Khan et al. (2022) investigated AgNPs synthesized from *Acer pentapomicum* using SEM. Their study found that the average size of AgNPs ranged from 19 to 25 nm and their shape was spherical. Ghabban et al. (2022), using SEM, found that AgNPs produced from *Astragalus spinosus* were spherical in shape and 30–40 nm in size. Another study on green-synthesized AgNPs from *Areca catechu* using SEM also revealed that the nanoparticles were spherical in shape (Choi et al., 2021). However, AgNPs synthesized from *Allium cepa* L. plant were in cubic shape (Abdellatif, 2022).

In the shape morphology of silver nanoparticles, icosahedron (polyhedron) and leaf-shaped particles were found (Choi et al., 2021). SEM images also revealed that the silver nanoparticles were highly aggregated at some points, which may be due to the magnetic behavior of the silver nanoparticles, and their larger surface area to volume ratio tends to concentrate them to reduce the surface energy (Khan et al., 2022). To eliminate agglomeration, these particles can be coated with a biocompatible polymer (Ghabban et al., 2022).

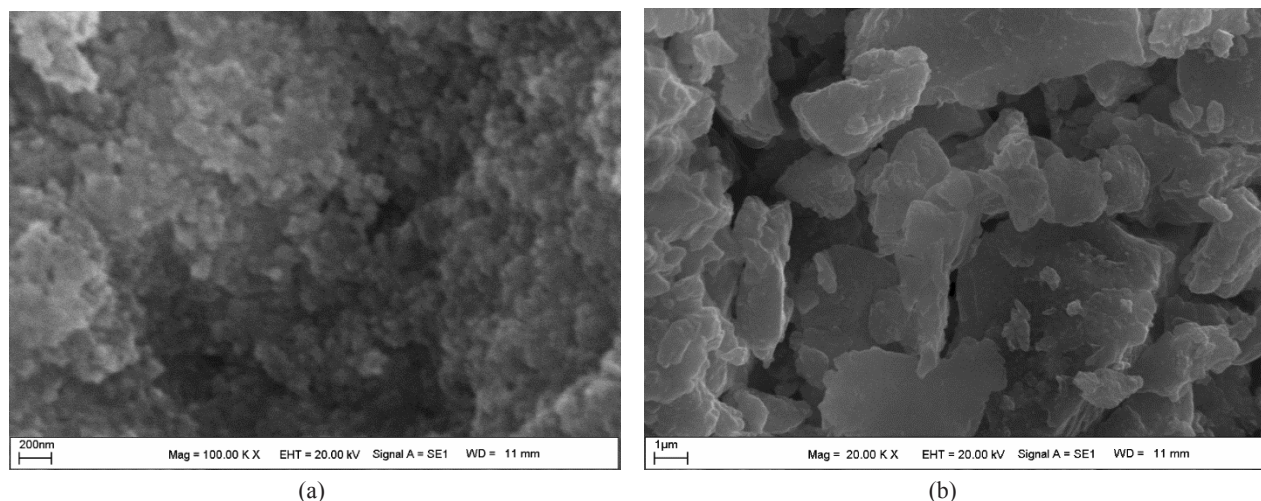


**Figure 1** – SEM results of AgNPs obtained by *Artemisia lerchiana* Web. plant extract in various scales

### TEM Analysis

TEM makes the atomic scale visible since it is more powerful than optical microscopes that rely on visible light to achieve a magnification of 50 million nanometer objects. The topography and dimension of green-synthesized *Artemisia lerchiana* are discussed. The TEM analysis was done to characterize AgNPs.

EM images of low and high resolution showed that nanoparticles were highly stable in nature, of small size, monodisperse and spherical in shape, and had smooth surfaces with no agglomeration. The TEM images were obtained at a scale bar of 50 nm to give the size reference of AgNPs and average particle size of 4–19 nm (Figure 2).

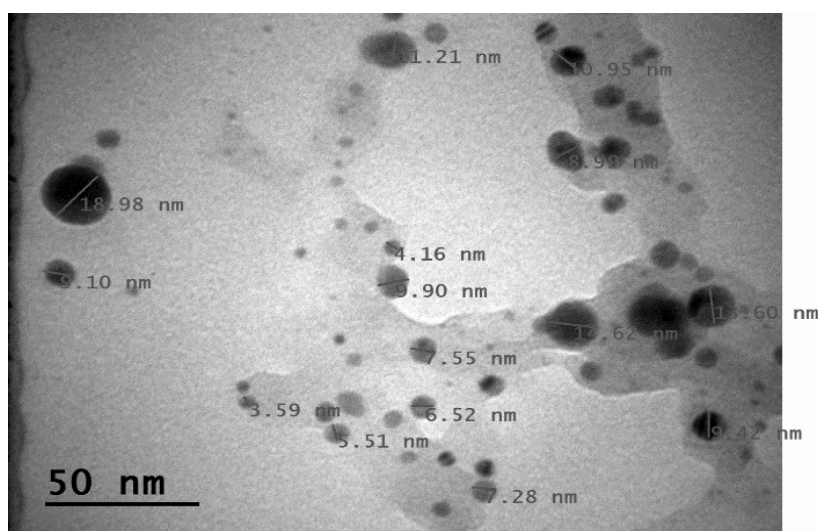
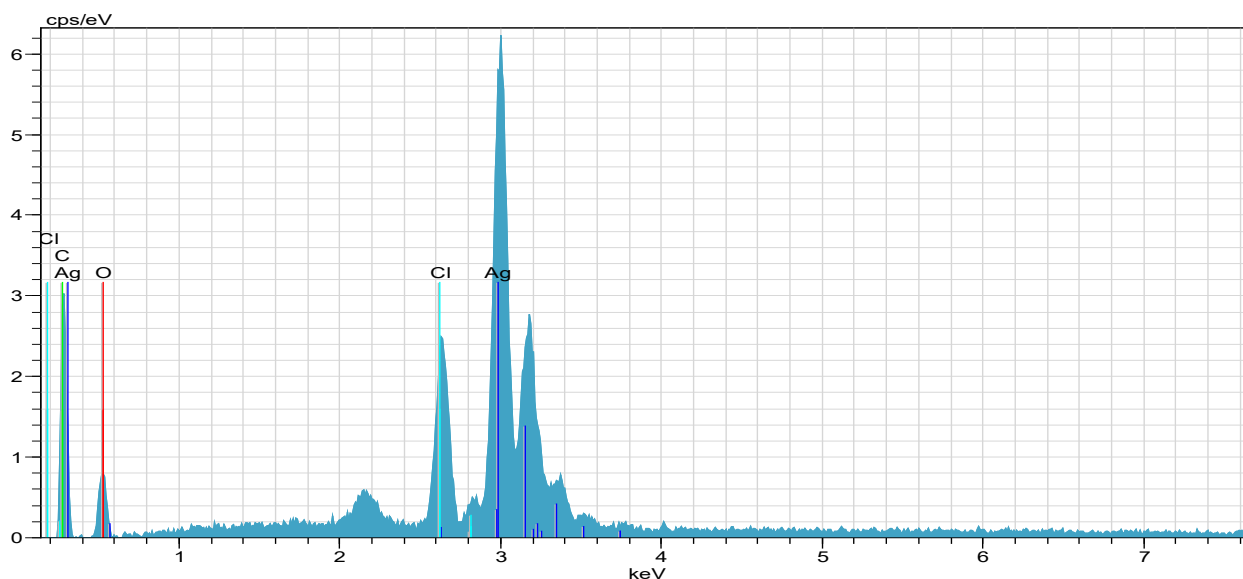


**Figure 2** – TEM image of AgNPs obtained from *Artemisia Lerchiana* plant extract at 50 nm

### Energy Dispersive X-ray Analysis (EDX)

The EDX spectrum revealed strong signals indicating the presence of Ag atoms in the biosynthesized *Artemisia lerchiana* Web. plant extract nanomaterial. The presence of elements carbon, chlorine,

and oxygen, which are sources of weak signals in the spectrum, was due to the plant extract. As reported in many studies with various plants, AgNPs showed a characteristic optical absorption peak at about 3 KeV depending on the SPR (Figure 3).



Element (El)	AN	Series	unn. C [wt.%]	norm. C [wt.%]	Atom. C [at.%]	Error [%]
Ag	47	L-series	53.69	64.35	18.85	2.5
C	6	K-series	14.38	17.24	45.37	2.7
Cl	17	K-series	0.46	0.55	0.49	0.1
O	8	K-series	14.90	17.86	35.29	3.1
<b>Total</b>	–	–	<b>83.44</b>	<b>100.00</b>	<b>100.00</b>	–

**Figure 3** – EDX analysis of AgNPs obtained by *Artemisia lerchiana* Web. plant extract

EDX analysis is one of the widely used methods by other authors. Thus, aqueous *Abutilon indicum* leaf extract was used for the biosynthesis of AgNPs, and EDX analysis presented a strong signal of Ag at 2.7 KeV (Ullah et al., 2021). Mani et al. (M. Mani et al., 2021) used *Cleome gynandra* leaf extract for the green synthesis of silver oxide nanoparticles and reported a similar type of spectrum. Vinay et al. (S.P. Vinay et al., 2019) used cow urine for the green synthesis of silver oxide nanoparticles and reported the same type of spectrum.

#### ***X-ray Diffraction (XRD) Analysis***

An intense peak at  $2\theta$   $38.04^\circ$  was chosen to calculate the crystal size, where  $K$  is the Scherrer constant,  $\lambda$  is the wavelength of the light used for diffraction,  $\beta$  is the FWHM value of the peak, and  $\theta$  is the Bragg angle. The Scherrer constant ( $K$ ) in the

formula above takes into account the shape of the particle and is generally taken to have a value of 0.9. As a result of calculations, it was determined that the average crystal size of silver nanoparticles is 24.83 nm (Figure 4).

According to the XRD spectrum data of *Artemisia Lerchiana*-AgNPs, the diffraction peaks are at  $27.77^\circ$ ,  $32.14^\circ$ ,  $38.04^\circ$ ,  $44.29^\circ$ ,  $46.18^\circ$ ,  $54.79^\circ$ ,  $57.4^\circ$ ,  $64.40^\circ$ , and  $77.36^\circ$ , which indicates that silver is cubic and represents the crystal structure in the  $2\theta$  plane (index).

Peaks representing the crystal structure of silver have been reported in many herbal silver nanoparticle synthesis studies such as *Cinnamomum camphora* (Aref & Salem, 2020), *Crossopteryx febrifuga*, *Brillantaisia patula*, *Senna siamea* (Kambale et al., 2020), *Cicer arietinum* (Baran et al., 2022), and *Prunus dulcis* (Aktepe et al., 2021).

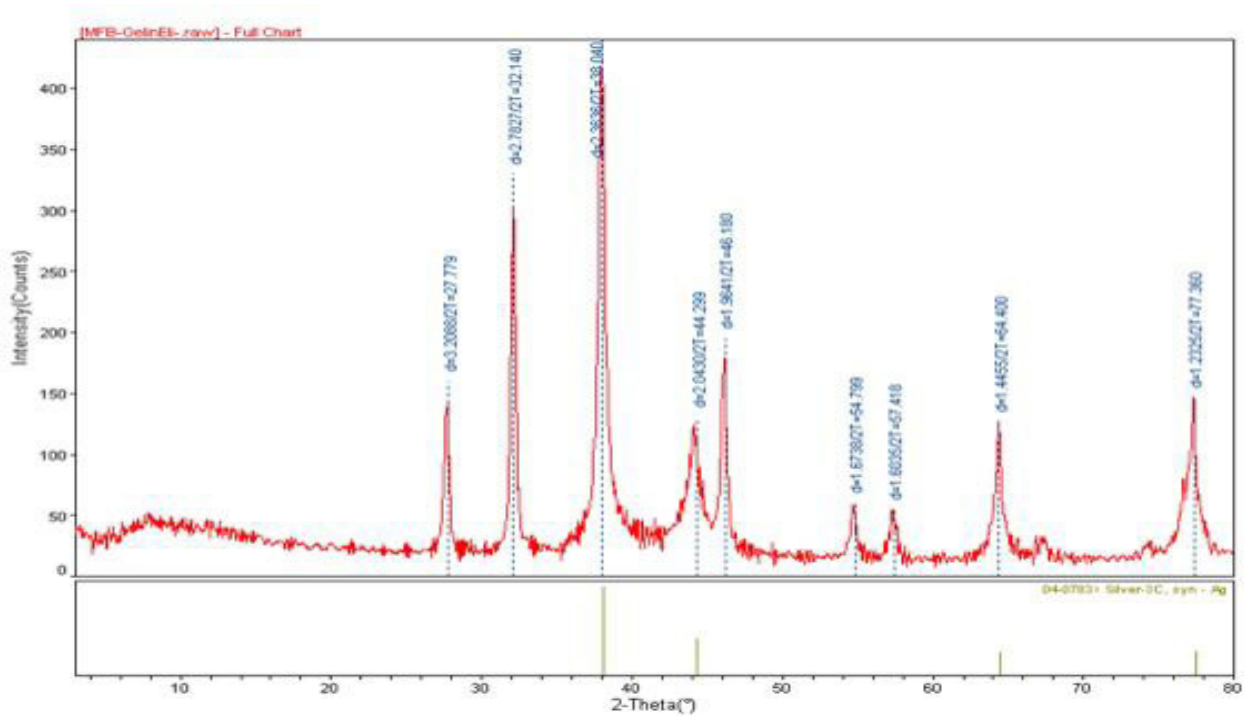


Figure 4 – XRD analysis of AgNPs obtained by *Artemisia lerchiana* Web. plant extract

**TG and DTA Analysis**

According to the research, 18.7% mass loss occurred in the sample at a temperature ranging from 200°C to 390°C, and 20.6% at a temperature ranging from 390°C to 731°C. Mass loss occurred mostly

at temperatures ranging from 390°C to 731°C (Figure 5). These mass losses simply indicate a slow degradation of the nanomaterial, suggesting that the resulting AgNPs are stable even at high temperatures.

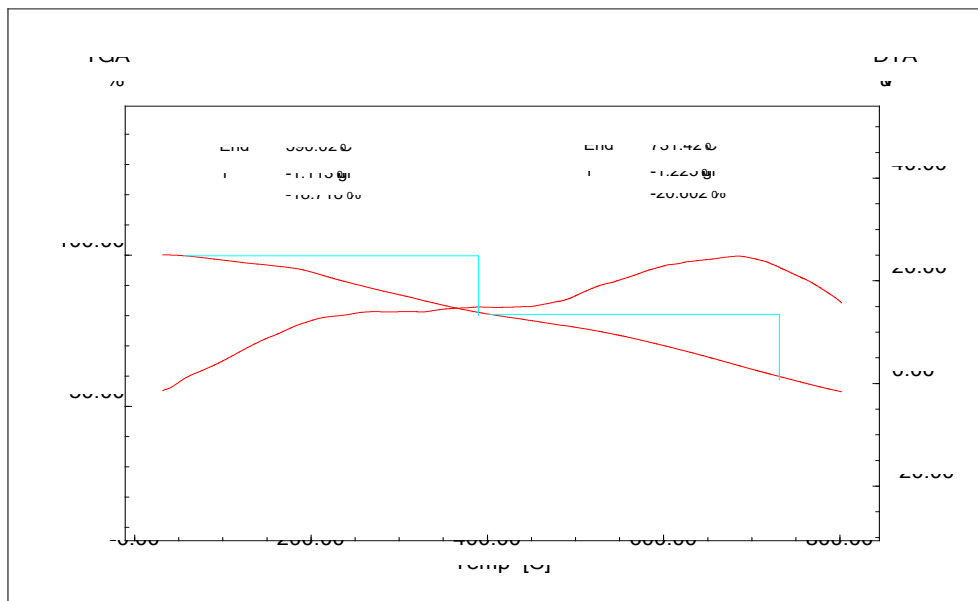
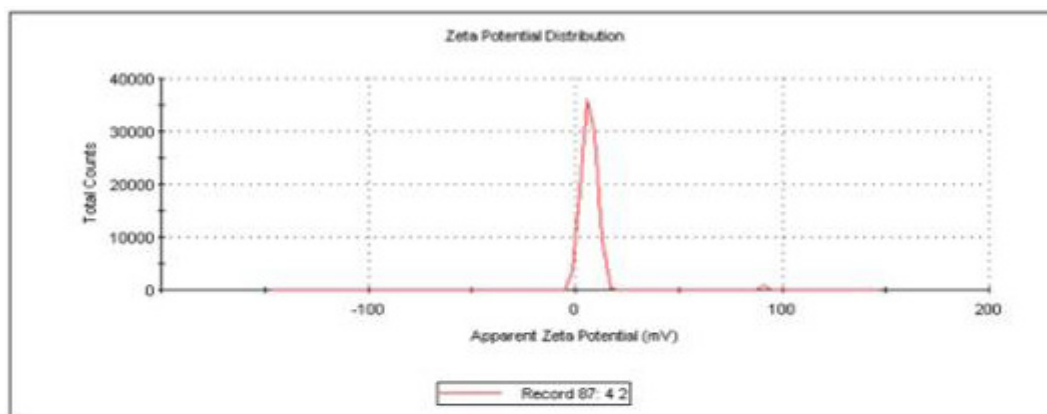


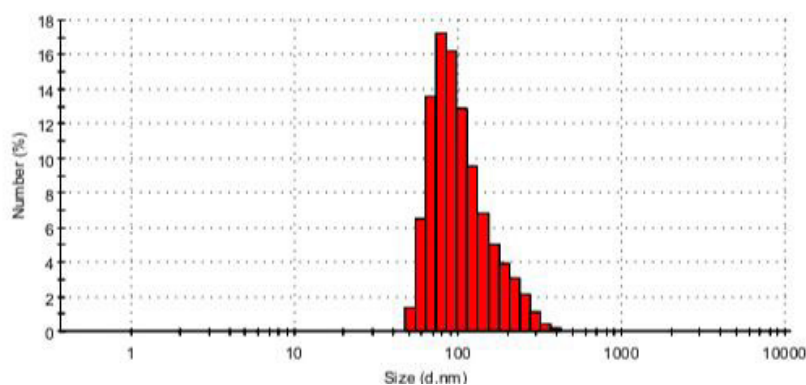
Figure 5 – TG-DTA results of AgNPs synthesized via wormwood extract

analysis of the zeta size and zeta potential was done to ascertain the surface charges and size distributions of the biosynthesized AgNPs, and it was determined that AgNPs featured a surface charge of  $-20$  mV (Fig. 6). A negative zeta potential is often attributed to the presence of capping phytochemicals on the nanoparticle surface, which prevents aggregation and supports long-term colloidal stability. The

synthesis of nanoparticles cannot be done in a standard size, and nanoparticles with different sizes can be produced. The mean sizes of nanoparticles have been found to be 27–32, 59.74, and 510 nm in numerous investigations (Al Ogaidi et al., 2017). It could be because the negative zeta potential of AgNPs indicates that they are a stable substance with non-sticking particles.



(a)



(b)

**Figure 6** – Physicochemical characterisation of biosynthesized AgNPs:

- (a) Zeta potential analysis indicating a surface charge of  $-20$  mV, suggesting colloidal stability.  
 (b) Dynamic light scattering (DLS)- based particle size analysis showing an average size distribution of 165 nm

AgNPs synthesized under a greener approach have a superior negative charge distribution compared to other conventional (chemical and physical) synthesis methods. According to studies, several plants—*Andrographis paniculata* (Prabhu & Poulose, 2012), *Convolvulus arvensis*, and *Matricaria chamomilla* (Rasheed et al., 2018)—exhibit surface charge and zeta potential distributions of 136 nm,  $-26$  mV; 68.06 nm,  $-21.4$  mV; and 90.9 nm, respectively.

## Conclusion

The present study successfully demonstrated the green synthesis of silver nanoparticles (AgNPs) using *Artemisia lerchiana* Web. plant extract as an eco-friendly reducing and stabilizing agent. The biosynthesis approach proved efficient, rapid, and sustainable, producing nanoparticles without the need for toxic chemicals or high-energy procedures. Vi-

sual color change during the reaction indicated the reduction of  $\text{Ag}^+$  to  $\text{Ag}^0$ , and subsequent characterization confirmed the successful formation of Ag-NPs. SEM analyses revealed predominantly spherical nanoparticles with sizes ranging from 25–50 nm, while TEM images showed more detailed nanoscale morphology with smooth, monodisperse particles in the size range of 4–19 nm. These differences in observed particle size likely result from agglomeration in the dried SEM samples versus individual dispersion under TEM analysis.

EDX spectroscopy verified silver as the major element, accompanied by carbon, oxygen, and chlorine originating from plant phytochemicals, thus confirming the purity and biosynthetic origin of the nanoparticles. XRD analysis showed distinct diffraction peaks corresponding to the face-centered cubic (fcc) crystalline structure of silver, and the calculated

crystallite size (24.83 nm) further supported the formation of nanoscale material. Thermal (TG–DTA) evaluation demonstrated good thermal stability, suggesting that the nanoparticles maintain structural integrity even at elevated temperatures. Zeta potential measurements indicated a negative surface charge (–20 mV), attributed to phytochemical capping, which is consistent with long-term colloidal stability and reduced aggregation.

Overall, the results confirm that Artemisia lerchiana extract is a highly effective bio-reducing agent for producing stable, crystalline AgNPs. The synthesized nanoparticles exhibit desirable physicochemical properties, indicating their potential applicability in antimicrobial, catalytic, biomedical, and environmental systems. This green synthesis method offers a promising pathway toward sustainable nanomaterial production.

### References

1. Thirumurugan A., Aswitha P., Kiruthika C., Nagarajan S., Christy A.N. (2016) Green synthesis of platinum nanoparticles using *Azadirachta indica* an eco-friendly approach. *Mater. Lett.*, vol. 170, pp. 175–178.
2. Abdellatif et al. (2022) Bioactivities of the green synthesized silver nanoparticles reduced using *Allium cepa* L aqueous extracts induced apoptosis in colorectal cancer cell lines.
3. Aktepe N., Baran A., Atalar M.N., Baran M.F., Keskin C., Düz M.Z., Yavuz Ö., İrtegünKandemir S., Kavak D.E. (2021) Biosynthesis of black mulberry leaf extract and silver nanoparticles: characterization, antimicrobial and cytotoxic activity. *MAS J. Appl. Sci.*, vol. 6, pp. 685–700.
4. Aref M.S., Salem S.S. (2020) Bio-callus synthesis of silver nanoparticles, characterization, and antibacterial activities via *Cinnamomum camphora* callus culture. *Biocatal. Agric. Biotechnol.*, vol. 27, 101689.
5. Al Ogaidi I., Salman M.I., Mohammad F.I., et al. (2017) Antibacterial and cytotoxicity of silver nanoparticles synthesized in green and black tea. *World J. Exp. Biosci.*, vol. 12, no. 1, pp. 39–45.
6. Baran A., Firat Baran M., Keskin C., Hatipoğlu A., Yavuz Ö., İrtegünKandemir S., Adican M.T., Khalilov R., Mammadova A., Ahmadian E., et al. (2022) Investigation of antimicrobial and cytotoxic properties of silver nanoparticles derived from *Cicer arietinum* L. *Front. Bioeng. Biotechnol.*, vol. 10, 855136.
7. Chellamuthu C., Balakrishnan R., Patel P., Shanmuganathan R., Pugazhendhi A., Ponnuchamy K. (2019) Gold nanoparticles using red seaweed *Gracilariaverrucosa*: green synthesis, characterization and biocompatibility studies. *Process Biochem.*, vol. 80, pp. 58–63.
8. Pandian C.J., Palanivel R., Dhananasekaran S. (2015) Green synthesis of nickel nanoparticles using *Ocimum sanctum* and their application in dye adsorption. *Chin. J. Chem. Eng.*, vol. 23, no. 8, pp. 1307–1315.
9. Devatha C.P., Thalla A.K., Katte S.Y. (2016) Green synthesis of iron nanoparticles using different leaf extracts for treatment of domestic wastewater. *J. Clean Prod.*, vol. 139, pp. 1425–1435.
10. Chernousova S., Epple M. (2013) Silver as antibacterial agent: ion, nanoparticle, and metal. *Angew. Chem. Int. Ed.*, vol. 52, pp. 1636–1653. <https://doi.org/10.1002/anie.201205923>.
11. Choi H.C., Jung Y.J., Baek et al. (2021) Antibacterial activity of green-synthesized silver nanoparticles using *Areca catechu* extract.
12. Dada A.O., Adekola F.A., Odeunmi E.O. (2017) Zerovalent manganese for copper removal: synthesis, characterization and adsorption studies. *Appl. Water Sci.*, vol. 7, no. 3, pp. 1409–1427.
13. Elumalai E.K., Prasad T.N.V.K.V., Hemachandran J., Therasa S.V., Thirumalai T., David E. (2010) Extracellular synthesis of silver nanoparticles using *Euphorbia hirta* leaves and their antibacterial activities.
14. Thema F.T., Manikandan E., Dhlamini M.S., Maaza M. (2015) Green synthesis of ZnO nanoparticles via *Agathosmabetulina* extract. *Mater. Lett.*, vol. 161, pp. 124–127.
15. Ghabban S.F., Alnomasy H., Almohammed et al. (2022) Antibacterial, cytotoxic and cellular mechanisms of green synthesized silver nanoparticles.
16. Kalishwaralal K., Vaidyanathan R., Venkataraman D., Pandian S.R., Muniyandi J., Hariharan N., Eom S.H. (2009) Biosynthesis, purification and characterization of silver nanoparticles using *Escherichia coli*. *Colloids Surf. B Biointerfaces*, vol. 74, pp. 328–335. <https://doi.org/10.1016/j.colsurfb.2009.07.048>.

17. Gurunathan S., Park J.H., Han J.W., Kim J.H. (2015) Apoptotic potential of silver nanoparticles synthesized by *Bacillus tequilensis* and *Calocybe indica*. *Int. J. Nanomed.*, vol. 10, pp. 4203–4222.
18. Kambale E.K., Nkanga C.I., Mutonkole B.-P.I., et al. (2020) Green synthesis of antimicrobial silver nanoparticles using Congolese plant species. *Heliyon*, vol. 6, e04493.
19. Khan Z.M., Almarhoon J., Bakht et al. (2022) *Acer pentapomicum*-mediated green synthesis of silver nanoparticles and evaluation of antimicrobial and antioxidant activities.
20. Lavoie et al. (1995) Environmental scanning electron microscopy of marine aggregates. *J. Microsc.*, vol. 178, no. 2, pp. 101–106.
21. Li L., Hu J., Yang W., Alivisatos A.P. (2001) Band gap variation in size- and shape-controlled CdSe quantum rods. *Nano Lett.*, vol. 1, pp. 349–351.
22. Li W.R., Xie X.B., Shi Q.S., et al. (2010) Antibacterial activity and mechanism of silver nanoparticles on *E. coli*. *Appl. Microbiol. Biotechnol.*, vol. 85, pp. 1115–1122.
23. Bandeira M., Giovanela M., Roesch-Ely M., Devine D.M., da Silva C.J. (2020) Green synthesis of ZnO nanoparticles: methodology and mechanism. *Sustain. Chem. Pharm.*, vol. 15, 100223.
24. Hosny M., Fawzy M., Abdulfetah A.M., Fawzy E.E., Eltaweil A.S. (2021) Green synthesis of gold nanoparticles using halophilic species: anticancer and catalytic efficiencies. *Adv. Powder Technol.*, vol. 32, no. 9, pp. 3220–3233.
25. Soliman M., Qari S.H., Abu-Elsaoud A., et al. (2020) Rapid green synthesis of silver nanoparticles enhances plant growth via antioxidant modulation. *Acta Physiol. Plant.*, vol. 42, no. 9, pp. 1–16.
26. Mani M., Harikrishnan R., Purushothaman P., Pavithra S., Rajkumar P., Kumaresan S., et al. (2021) Systematic green synthesis of silver oxide nanoparticles for antimicrobial activity. *Environ. Res.*, vol. 202, 111627.
27. Mukherjee P., Ahmad A., Mandal D., et al. (2001) Fungus-mediated synthesis of silver nanoparticles. *Nano Lett.*, vol. 1, pp. 515–519.
28. Aktepe N., Baran A. (2021) Fast and low-cost biosynthesis of AgNPs with almond leaves. *Prog. Nutr.*, vol. 23, no. 3, e2021271.
29. Clarence P., Luvankar B., Sales J., et al. (2020) Green synthesis of gold nanoparticles using *Fusarium solani* and biomedical applications. *Saudi J. Biol. Sci.*, vol. 27, no. 2, pp. 706–712.
30. Patra J.K., Gitishree D., Baek K.H. (2016) Phyto-mediated biosynthesis of AgNPs using watermelon rind extract: antibacterial and antioxidant efficacy. *J. Photochem. Photobiol. B.*, vol. 161, pp. 200–210.
31. Prabhu S., Poulouse E.K. (2012) Silver nanoparticles: antimicrobial mechanism and toxicity. *Int. Nano Lett.*, vol. 2, pp. 1–10.
32. Rai (2013) Green nanobiotechnology: biosynthesis of metallic nanoparticles and antimicrobial applications. *Ciência e Cultura*, vol. 65, no. 3, pp. 44–48.
33. Rasheed T., Bilal M., Li C., et al. (2018) Catalytic degradation of pollutants using biosynthesized silver nanoparticles. *J. Photochem. Photobiol. B.*, vol. 181, pp. 44–52.
34. Reverberi M., Voccianta M., Salerno M., Ferretti B., Fabiano B. (2019) Green synthesis of silver nanoparticles by low-energy bead milling.
35. Salem S.S., El-Belely E.F., Niedbala G., et al. (2020) Bactericidal and cytotoxic efficacy of silver nanoparticles fabricated by endophytic actinomycetes. *Nanomaterials*, vol. 10, p. 2082.
36. Vinay S.P., Nagaraju G., Chandrappa C.P., Chandrasekhar N. (2019) Cow-urine mediated synthesis of silver oxide nanoparticles. *J. Sci. Adv. Mater. Dev.*, vol. 4, pp. 392–399.
37. Saravanakumar M.M., Peng M., Ganesh M., Jayaprakash J., Mohankumar M., Jang H.T. (2017) Green synthesis of AgNPs using *Prunus japonica* and evaluation of antibacterial and antioxidant properties.
38. Sharma V.K., Yngard R.A., Lin Y. (2008) Silver nanoparticles: green synthesis and antimicrobial activities. *Adv. Colloid Interface Sci.*, vol. 145, pp. 83–96.
39. Badeggi U.M., Ismail E., Adeloye A.O., et al. (2020) Green synthesis of gold nanoparticles capped with procyanidins: anti-diabetic potential. *Biomolecules*, vol. 10, p. 452.
40. Ullah S., Noman M., Ali K.S., et al. (2021) Biosynthesis of AgNPs using *Abutilon indicum* leaf extract. *IOSR J. Environ. Sci. Toxicol. Food Technol.*, vol. 15, no. 1, pp. 4–14. <https://doi.org/10.9790/2402-1501010414>.
41. Cittrarasu V., Kaliannan D., Dharman K., et al. (2021) Green synthesis of selenium nanoparticles from *Ceropegia bulbosa*: antimicrobial and photocatalytic activities. *Sci. Rep.*, vol. 11, p. 1032.
42. Sunderam V., Thiyagarajan D., Lawrence A.V., Mohammed S.S., Selvaraj A. (2019) Antimicrobial and anticancer properties of gold nanoparticles synthesized using *Anacardium occidentale* leaf extract. *Saudi J. Biol. Sci.*, vol. 26, no. 3, pp. 455–459.

**Information about author:**

Gunay Hasanova – Baku State University, Z. Khalilov 23, Baku AZ1148, Azerbaijan.